The Journal of Neuroscience, September 1, 1996, *16*(17):5443–5456

Traffic of Dynamin within Individual *Drosophila* Synaptic Boutons Relative to Compartment-Specific Markers

Patricia S. Estes,[1] Jack Roos,[2] Alexander van der Bliek,[3] Regis B. Kelly,[2] K. S. Krishnan,[4] and Mani Ramaswami[1]

[1]*Department of Molecular and Cellular Biology and Arizona Research Labs, Division of Neurobiology, University of Arizona, Tucson, Arizona 85721,* [2]*Department of Biochemistry and Biophysics and Hormone Research Institute, University of California at San Francisco, San Francisco, California 94143-0534,* [3]*Department of Biological Chemistry, University of California at Los Angeles, Los Angeles, California 90024, and* [4]*Molecular Biology Unit, Tata Institute for Fundamental Research, Colaba, Bombay 400005, India*

Presynaptic terminals contain several specialized compartments, which have been described by electron microscopy. We show in an identified *Drosophila* neuromuscular synapse that several of these compartments—synaptic vesicle clusters, presynaptic plasma membrane, presynaptic cytosol, and axonal cytoskeleton—labeled by specific reagents may be resolved from one another by laser scanning confocal microscopy. Using a panel of compartment-specific markers and *Drosophila shibire*^{ts1} mutants to trap an intermediate stage in synaptic vesicle recycling, we have examined the localization and redistribution of dynamin within single synaptic varicosities at the larval neuromuscular junction. Our results suggest that dynamin is not a freely diffusible molecule in resting nerve terminals; rather, it appears localized to synaptic sites by association with yet uncharacterized presynaptic components. In *shi*^{ts1} nerve terminals depleted of synaptic vesicles, dynamin is quantitatively redistributed to the plasma membrane. It is not, however, distributed uniformly over presynaptic plasmalemma; instead, fluorescence images show "hot spots" of dynamin on the plasma membrane of vesicle-depleted nerve terminals. We suggest that these dynamin-rich domains may mark the active zones for synaptic vesicle endocytosis first described at the frog neuromuscular junction.

Key words: neurogenetics; endocytosis; membrane traffic; ultrastructure; temperature-sensitive paralysis; synaptic vesicle recycling; neurotransmitter release

Intercellular communication in the nervous system occurs primarily at chemical synapses. The most dramatic phenomenon at nerve terminals is the coupling of electrical depolarization to synaptic vesicle fusion. After fusion, synaptic vesicle membrane is internalized and recycled to form new synaptic vesicles. The speed and high fidelity of these processes are accomplished by a large number of presynaptic proteins with highly specific spatial localizations (Burns and Augustine, 1995; Sudhof, 1995). Several components of the presynaptic machinery required for synaptic vesicle exocytosis have been identified, and detailed models exist for their potential roles in transmitter release (Bennett and Scheller, 1993; Sollner et al., 1994). Good models for molecular mechanisms involved in synaptic vesicle traffic make strong predictions for the precise localization of identified components of the presynaptic machinery. Some of these predictions, such as the specific localization of the t-SNARE syntaxin to fusion sites on the presynaptic plasma membrane, have been proved incorrect by subsequent careful experiments. Syntaxin is found not only on axonal membrane far from the sites of transmitter release but also on synaptic vesicle membrane (Garcia et al., 1995; Schulze et al., 1995). Thus, for a deep understanding of presynaptic mechanisms, it is important to localize identified molecules at a fine level within the nerve terminal.

The nerve terminal is not a static structure. Transient calcium influxes are coupled to synaptic vesicle fusion events. Vesicle collapse into plasma membrane probably results in the lateral diffusion of synaptic vesicle proteins (Heuser and Reese, 1973). Subsequently, synaptic vesicle membrane is retrieved by an endocytotic mechanism, and recycled synaptic vesicles, perhaps generated from an intermediate endosome, are actively mixed with a reserve pool of transmitter-filled vesicles (Heuser and Reese, 1973; Sudhof, 1995; Betz and Wu, 1995). Various proteins involved in these processes must actively redistribute between several presynaptic compartments during the synaptic vesicle cycle. To completely understand the function of each presynaptic protein, it would be useful to know its location during every step of the synaptic vesicle cycle. This is of special significance for proteins without membrane-anchoring sequences, as no obvious thermodynamic barriers exist to restrict their spatial distribution. Such localization studies require a nerve terminal preparation accessible to electrophysiology and large enough for good microscopic

Received April 30, 1996; revised June 11, 1996; accepted June 12, 1996.

This work was funded by a National Science Foundation grant to M.R. and National Institutes of Health grants to A.v-d.B. and R.B.K. J.R. is a postdoctoral fellow supported by National Institutes of Health Training Grant T32-HD07397. M.R. is a Sloan Research Fellow and a McKnight Neuroscience Scholar. We thank Christos Consoulas from Richard Levine's lab for introducing us to the biocytin fill technique. We acknowledge Patty Jansma for patient assistance with electron microscopy and for her efficient management of the Arizona Research Labs (ARL) microscopy facility, Gina Zhang of the EM Core Facility at the University of Arizona's Department of Anatomy for thin sections, and Charles (Chip) Hedgcock, Registered Biological Photographer, for help with EM micrographs. Most of the microscopy was performed using a Bio-Rad 600 confocal microscope and a Jeol 200EX electron microscope belonging to the ARL Division of Neurobiology. We thank Troy Littleton and Hugo Bellen for anti-syt antibodies, Erich Buchner and Konrad Zinsmaier for anti-csp antibodies, and Seymour Benzer for the monoclonal antibody 22C10. This manuscript was improved substantially by comments from Sam Ward, Jane Robinson, Alison Adams, members of the Ramaswami lab, and an anonymous reviewer.

Correspondence should be addressed to Mani Ramaswami, Department of Molecular and Cellular Biology, Life Sciences South, University of Arizona, Tucson, AZ 85721.

studies, where several presynaptic molecules have been identified, and in which individual transient stages in the dynamic synaptic vesicle cycling pathway may be trapped and analyzed. Although no synapse exists that meets all of these conditions, we provide evidence in this paper to suggest that motor terminals on *Drosophila* larval bodywall muscles meet several of these requirements.

The accessibility of identified synapses to morphological and electrophysiological analyses at all stages in development has made the *Drosophila* larval neuromuscular junction an increasingly important preparation for the analysis of synapse formation and function. Thus, the analysis of *Drosophila* mutant synapses bearing null or partial loss of function mutations in various genes encoding presynaptic molecules has yielded many unique insights into the molecular mechanisms of transmitter release (Bate and Broadie, 1995). A little-used feature of fly larval motor terminals is their relatively large size. Type 1b varicosities on the ventral longitudinal muscles 6 and 7 are usually between 3 and 5 μm in size and sometimes are even larger (Johansen et al., 1989; Atwood et al., 1993; Lahey et al., 1994). Thus, an individual presynaptic varicosity on these muscles may be the same size as an entire yeast cell, while being substantially less complex in the variety of cellular structures it contains. For this reason, significant morphological detail within resting *Drosophila* presynaptic boutons is discernible by optical microscopic methods (Lahey et al., 1994; Ramaswami et al., 1994). An otherwise transient intermediate stage during synaptic vesicle recycling may be trapped using the *Drosophila shibire*^{ts1} mutation, which causes temperature-sensitive paralysis in larval and adult flies (Kosaka and Ikeda, 1983; Ramaswami et al., 1994). The *shibire* (*shi*) gene encodes dynamin, a GTPase essential for synaptic vesicle recycling; the *shi*^{ts1} mutation probably prevents GTP hydrolysis at elevated temperatures (Chen et al., 1991; van der Bliek and Meyerowitz, 1991; Damke et al., 1995; Takei et al., 1995) (see Discussion). Thus, stimulation of *shi*^{ts1} mutant terminals at nonpermissive temperatures traps synaptic vesicle membrane at a "collared-pit" stage in membrane internalization, probably just before the step requiring GTP hydrolysis by dynamin (Kosaka and Ikeda, 1983).

We have exploited the large size of *Drosophila* presynaptic varicosities and have used confocal microscopy to examine the relative localization of various compartment-specific markers at the nerve terminal. In resting nerve terminals, synaptic vesicles show a distribution pattern quite distinct from presynaptic plasma membrane, presynaptic cytosol, and the axonal cytoskeleton. The distribution of synaptic vesicle membrane proteins is dramatically altered, from an intracellular domain to plasma membrane, in *shi*^{ts1} mutant synapses depleted of synaptic vesicles (van de Goor et al., 1995). We have examined the distribution of *Drosophila* dynamin relative to our collection of presynaptic markers. In resting nerve terminals, dynamin is in an intracellular pool, but it does *not* show the same distribution as a soluble, freely diffusible molecule, as suggested by previous biochemical experiments (Robinson et al., 1994). Rather, dynamin seems to be associated with an uncharacterized presynaptic component, which may serve to prevent its diffusion from synaptic sites. In *shi*^{ts1} terminals that have been depleted of synaptic vesicles, dynamin is membrane-associated, as suggested previously (Robinson et al., 1994; Takei et al., 1995); however, our images show dynamin to be concentrated sharply at specific hot spots on presynaptic plasmalemma. These hot spots may correspond to active zones for synaptic vesicle membrane retrieval.

MATERIALS AND METHODS

Drosophila culture and stocks. Flies were cultured in standard sugar/agar-containing yeasted medium in vials or bottles at temperatures between 19 and 22°C. Oregon-R and *shi*^{ts1} mutants were from the Krishnan and Ramaswami laboratory stock collection (Ramaswami et al., 1994).

Larval bodywall muscle preparation. Third-instar larval neuromuscular preparations and the stereotypic pattern of innervation of larval bodywall muscles have been described previously (Jan and Jan, 1976; Johansen et al., 1989). Wandering third-instar larvae were picked off the walls of the bottles and dissected to expose their bodywall muscles. For dissection, the larva was placed dorsal side up on a 35-mm-diameter petri dish with a thin layer of Sylgard resin (Dow Corning, Corning, NY). The larval head was pinned to the Sylgard, and then the entire larva was immersed in calcium-free saline. The posterior tip of the larva was snipped away, and the entire larva was cut along the dorsal midline using fine microdissecting scissors (Fine Science Tools, Foster City, CA). The filleted larva was pinned out using fine insect pins (Fine Science Tools), and the viscera were removed gently. In the final preparation, segmentally repeated larval muscles innervated by axons from the CNS were clearly visible. The ventral longitudinal muscles (muscles 6 and 7) could be identified easily as the most superficial muscles visible in the preparation (Johansen et al., 1989; Bate, 1993; Broadie and Bate, 1993).

Organization and morphology of synaptic terminals on larval ventral longitudinal muscles. The organization and structure of synapses on the ventral longitudinal muscles have been described previously at the level of light and electron microscopy (Jan and Jan, 1976; Johansen et al., 1989; Atwood et al., 1993; Bate, 1993; Jia et al., 1993). Muscles 6 and 7 are innervated dually by two motor axons, termed Axon 1 and Axon 2 by Atwood et al. (1993), which form two morphologically and functionally distinct kinds of presynaptic varicosities, termed Type 1b (for big boutons) and Type 1s (for small boutons), on the target muscles (Atwood et al., 1993; Kurdyak et al., 1994). Under the light microscope, the two kinds of terminals may be distinguished by their size and by the length of axon in contact with muscle. Type 1s terminals are sized homogeneously (between 1.5 and 3 μm), whereas Type 1b terminals are more variable (2–6 μm), and Type 1s axons typically extend a greater distance along the muscle surface (Atwood et al., 1993; Jia et al., 1993; Ramaswami et al., 1994) (see Fig. 5). Under the electron microscope, the two kinds of boutons are differentiated by the extent of associated subsynaptic reticulum (specialized microvillar muscle membrane), by the relative richness of mitochondria in the terminals, and by the relative preponderance of larger vesicular structures within the presynaptic bouton. Type 1b terminals are associated with very well developed layers (up to 10) of subsynaptic reticulum (type 1s terminals have fewer than three layers) and have more mitochondria and fewer large vesicular structures (Atwood et al., 1993; Jia et al., 1993; Lahey et al., 1994). All detailed morphological experiments described in this paper were performed on the large Type 1b boutons found on muscles 6 and 7 of abdominal segments A2–A3. All neuromuscular preparations that we used had the CNS still attached.

Salines. Normal saline was 130 mM NaCl, 36 mM sucrose, 5 mM KCl, 5 mM HEPES, pH 7.3, 2 mM $MgCl_2$, and 2 mM $CaCl_2$ (Jan and Jan, 1976; Broadie and Bate, 1993); for calcium-free saline, $CaCl_2$ was replaced by 2 mM $MgCl_2$ and 0.5 mM EGTA; high-K^+ saline was 60 mM KCl, and external NaCl was reduced by an equivalent amount.

High-K^+ stimulation. Peripheral nerves of insect larvae are surrounded by a glial sheath that protects them from the high-K^+ (23 mM in *Drosophila*) concentration of the hemolymph (Stewart et al., 1994; Auld et al., 1995). Despite this apparent insulation, exposure of *Drosophila* larval neuromuscular preparations, with attached CNSs, to 60 mM K^+ saline induces membrane depolarization and synaptic activity at the ventral longitudinal muscles 6 and 7 (Ramaswami et al., 1994). High-K^+ stimulation was with 60 mM K^+ saline for 5 min at the specified temperature. After stimulation and before fixation, the high-K^+ saline was replaced briefly (~5 sec) with prewarmed calcium-free saline to relax the preparation.

Generation of antibodies. Rabbit anti-synaptotagmin (DSYT-2) antibody was a generous gift from Troy Littleton and Hugo Bellen (Baylor College of Medicine). Anti-CSP antibody (mAb49) was a gift from Erich Buchner (Universitat Wurzburg) and Konrad Zinsmaier (University of Pennsylvania School of Medicine). FITC-conjugated anti-HRP was purchased from Cappel (West Chester, PA), and monoclonal antibody 22C10 was a gift from Seymour Benzer's laboratory (California Insitute of Technology).

The rabbit antiserum, shi-3, was made against a KLH-conjugated 16 residue peptide from the C-terminal proline-rich sequence of *Drosophila*

dynamin (CRPGGSLPPPMLPSRR). The peptide was made at the Caltech peptide facility, conjugated to KLH, and sent to Pocano Rabbit Farms (Canadensis, Pennsylvania) for antibody production in rabbits. Polyclonal antibodies 2073 and 2074 to *Drosophila* dynamin were raised against purified recombinant fusion proteins. Fusion proteins used as immunogens were sent to Immuno-Dynamics (La Jolla, CA) for antibody production in rabbits. A 37 kDa fragment of *Drosophila* dynamin, encompassing amino acids 331–651 (which includes the pleckstrin homology domain of dynamin), was fused to glutathione-*S*-transferase (GST). This fusion protein was used to generate the serum Ab2073. A 66 kDa fragment of *Drosophila* dynamin, lacking the N-terminal 241 amino acids (lacking the GTP-binding domain), was fused to the maltose-binding protein (MBP) and used to generate the antiserum Ab2074.

Antibodies were affinity-purified by the method of Smith and Fisher (1984). Either GST-dynamin (for Ab2074) or MBP-dynamin (for Ab2073) was overexpressed in bacteria and recovered as a sarkosyl extract (Grieco et al., 1992). Fusion protein was subsequently resolved on an SDS-PAGE gel and transferred to nitrocellulose (Schleicher & Schuell, Keene, NH) using standard methods (Towbin et al., 1979). The nitrocellulose was stained briefly with 0.2% Ponceau S (Sigma, St. Louis, MO), and the nitrocellulose bearing the fusion protein was excised, diced, and placed in a 1.5 ml microfuge tube. The filter was blocked in PBS containing 0.05% Tween 20 and 1% BSA, washed with PBS containing 0.05% Tween 20 and 0.1% BSA, and then incubated with serum overnight. The nitrocellulose was washed three times with PBS/0.05% Tween 20/0.1% BSA and then eluted with 300 μl aliquots of 5 mM glycine, pH 2.3/500 mM NaCl/0.5% Tween 20/100 mg/ml BSA. The eluates, immediately neutralized with 15.75 μl of 1 M Na_2HPO_4, contained affinity-purified antibodies.

Western analysis. Drosophila head postnuclear supernatant (S1) was generated as described previously (van de Goor et al., 1995), except that ground heads were resuspended in 10 mM HEPES, pH 7.4/0.1 mM $MgCl_2$/1 mM $CaCl_2$ + protease inhibitors and homogenized by 20 strokes in a glass homogenizer using a drill press. Sample analysis was performed by resolving 15 mg S1 extract on 5–17.5% SDS-PAGE gels. The gels were electroblotted onto nitrocellulose, blocked with 3% nonfat dry milk powder in PBS/0.05% Tween 20, and incubated with a 1:1000 dilution of Ab2073, a 1:2000 dilution of Ab2074, or a 1:2500 dilution of shi-3 sera. Detection was accomplished with an HRP-conjugated secondary antibody (Cappel) and developed with an ECL detection system (Amersham, Arlington Heights, IL), according to the manufacturer's directions.

Immunohistochemistry. Synaptic vesicle markers DSYT-2 and mAb49 were used at 1:200 and 1:20 dilutions, respectively. The dynamin antiserum shi-3 was used at 1:200, and affinity-purified Ab2073 and Ab2074 were used at 1:200 and 1:500, respectively. Monoclonal antibody 22C10 and FITC-conjugated anti-HRP (Cappel) were used at a 1:50 dilution. Secondary antibodies were from Cappel: FITC or Texas Red-conjugated goat anti-rabbit (or goat anti-mouse) IgGs were used at a 1:200 dilution.

Previous work in adult neuromuscular preparation has shown that application of aldehyde fixative in the presence of calcium results in a burst of motor activity induced by CNS stimulation before complete fixation (Koenig et al., 1989). To avoid such confounding phenomena in our larval fillets, which had attached CNSs, we used calcium-free fixative containing 0.5 mM EGTA in our experiments. Preparations were fixed 30 min in freshly prepared 3.5% paraformaldehyde in Ca^{2+}-free PBS and washed. The preparation was first blocked with 5% goat serum and 2% BSA in PBS with 0.2% Triton X-100 (TBS) for 2 hr. Primary antibody in TBS was incubated for 2 hr and secondary was incubated for 1 hr at room temperature. The preparation was mounted in 0.1% paraphenylene diamine (Sigma) in 95% glycerol and viewed.

Biocytin fills of nerve terminals. Third-instar larvae were filleted as described earlier. The anterior anchors of the ventral ganglion were cut away, and the CNS was lifted into a conical Vaseline well made at the anterior end of the larva with a fine Vaseline dispenser. After the well contents were isolated from the bath, the CNS was either crushed or cut away in distilled water to expose the ends of the motor nerves to the contents of the well. The well was filled with saturated biocytin (Sigma) solution in distilled water, and the preparation was kept at room temperature for 3 hr. The preparation was washed in saline, fixed with 3.5% paraformaldehyde solution for 30 min, and subsequently stained with fluorescently conjugated streptavidin (Vector Labs, Burlingame, CA) to visualize biocytin-labeled structures. In general, with a 3 hr incubation, synapses on the anterior segments were stained more brightly, presumably because biocytin required less time to diffuse down the shorter motor nerves.

Optical microscopy and image processing. At least five experiments were conducted for each pair of antibodies, and at least six different hemisegments from each preparation were examined carefully. In general, the number of experiments greatly exceeded this number. For every experiment in which we examined redistribution of antigens in *shi*^{ts1} mutants after vesicle depletion, a wild-type preparation was processed similarly in parallel. Initially, the preparations were labeled in code by one of us and examined "blind" by the other, under a conventional fluorescence microscope. We found that *shi*^{ts1} preparations could be identified easily in every case (more than 10 were tested blind): *shi*^{ts1}-depleted terminals appeared to be swollen, boutons boundaries were not as distinct, and synaptic vesicle membrane markers appeared to label the axonal plasma membrane. In wild-type or in resting, unstimulated *shi*^{ts1} terminals, synaptic vesicle proteins were never found in the ring-like structures shown in Figures 2*C,D*, 3*C,D*, and 7, but rather were found in a compact and dense pattern within presynaptic varicosities. To compare biocytin or dynamin localization with synaptic vesicle markers, we selected boutons to examine in the following manner. For *shi*^{ts1}-depleted terminals, we generally looked at synaptic vesicle protein localization through one filter and chose fields of view in which the best optical sectioning could be achieved; in these ideally oriented varicosities, we examined the localization of the second marker. It was not always possible in *shi*^{ts1} preparations to mark clearly the beginning and end of the presynaptic varicosities, perhaps because of swelling of adjacent axonal regions connecting the varicosities. For wild-type terminals in which varicosities were clearly visible, we preferred to analyze terminal synapses on the muscle surface where good optical sectioning was possible. Little additional information was obtained from three-dimensional reconstructions.

We used a Bio-Rad 600 laser-scanning confocal microscope (Bio-Rad, Richmond, CA) and the COMOS software package to acquire all fluorescence images shown in this paper. For FITC and Texas Red double-labeled preparations, images were acquired simultaneously using the K1/K2 filters provided by Bio-Rad. For all of our experiments, we ensured that fluorescence bleedthrough was not a significant problem. To acquire the thin optical sections shown in most of the figures, the aperture was generally set at 0.4, and a 60× 1.4 NA lens was used at high zoom (generally 6). We took Z series where the focal planes were stepped by 0.5–1.0 μM between successive images. The brightest optical section containing most of the immunoreactivity was selected in every case. The split-screen images acquired from the confocal microscope were split exactly into two using a National Institutes of Health Image macro provided by Dr. ChiBin Chien from the University of California San Diego. The split red and green images were scaled independently (linearly) to equal maximal brightness using National Institutes of Health Image. No further processing of the images occurred. National Institutes of Health Image files were subsequently imported into Adobe Photoshop for generation of the red–green overlays shown in the figures.

Electron microscopy. We examined approximately 20 presynaptic boutons on muscles 6 and 7 in abdominal segment A2 or A3 in three *shi*^{ts1} and two wild-type larvae. After wild-type and *shi*^{ts1} larvae neuromuscular preparations were stimulated at elevated temperatures, they were fixed for 30 min at 34°C, followed by 90 min at room temperature, and overnight at 4°C in freshly prepared fixative containing 4% paraformaldehyde (Sigma) and 1% or 6% glutaraldehyde (Sigma) in 100 mM cacodylate buffer, pH 7.2, 2 mM sucrose, and 0.5 mM EGTA. After fixation, the tissue was rinsed three times in 100 mM cacodylate buffer with 264 mM sucrose. Right and left hemisegments from A2 and A3 were separated from the larval fillet at this stage and postfixed with 1% OsO_4 in 100 mM cacodylate buffer for 2 hr. Some preparations were stained *en bloc* for 1 hr (the *shi* preparation shown was not stained *en bloc*) with 1% uranyl acetate in 70% EtOH before dehydration in an ethanol series. The tissue was embedded in Epon (Embed 812; Electron Microscopy Sciences), and longitudinal ultrathin sections were made on an LKB ultramicrotome using a diamond knife. Grids were poststained with 2% uranyl acetate and 1% lead citrate and examined with a Jeol 1200EX electron microscope.

RESULTS

High-temperature stimulation depletes synaptic vesicles in larval shi^{ts1} Type 1b terminals

Previous electron microscopic (EM) studies on synaptic vesicle depletion in *shi* mutants have been performed at adult synapses, which are not as convenient as larval synapses for studies of synaptic transmission. To establish that *shi*^{ts1} larval nerve termi-

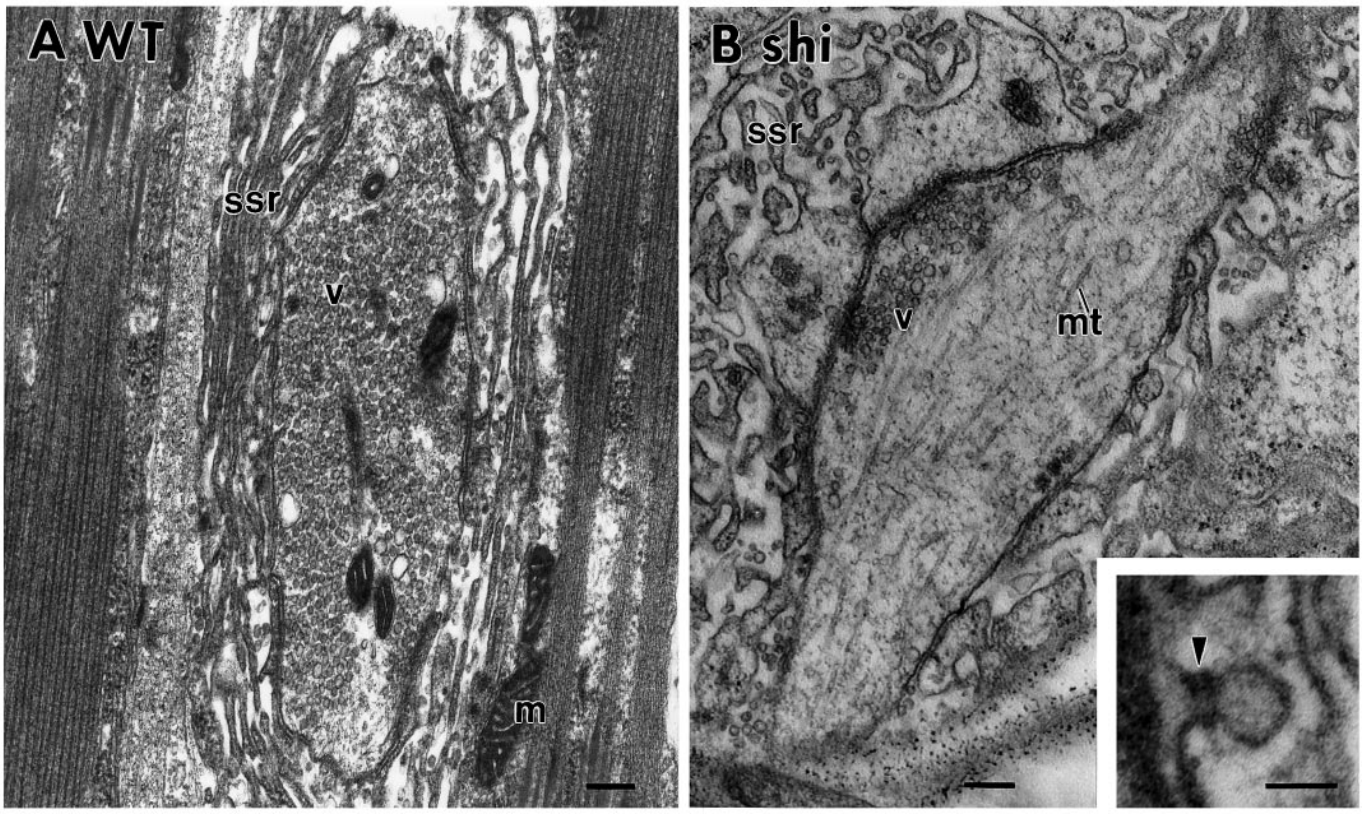

Figure 1. Synaptic vesicles are depleted in type 1b synaptic varicosities of *shi*^{ts1} larval muscles 6 and 7 by high-K^+ stimulation at elevated temperatures. *A*, Synaptic vesicles are not depleted in a control wild-type synaptic bouton stimulated for 5 min at 34°C. *B*, Vesicles are depleted in identically stimulated *shi*^{ts1} nerve terminals. The *inset* shows a collared pit trapped in the *shi*^{ts1} larval terminal. *m*, Mitochondrion; *ssr*, subsynaptic reticulum; *v*, synaptic vesicle; *mt*, microtubule. *Arrowhead* indicates a collar on the nascent endocytotic vesicle. Scale bars: *A, B*, 200 nm; *inset*, 50 nm.

nals may be arrested similarly at a specific stage in synaptic vesicle recycling, we used EM studies to examine the ultrastructure of wild-type and *shi*^{ts1} larval type Ib synaptic boutons on the ventral longitudinal muscles 6 and 7 after high-K^+ stimulation at elevated temperatures.

Under the electron microscope, a substantial depletion of synaptic vesicles was observed in *shi*^{ts1} but not in control, wild-type terminals stimulated at 34°C. Figure 1, *A* and *B*, shows the typical wild-type and *shi*^{ts1} terminals that we observed. As in adult *shi*^{ts1} animals, larval *shi*^{ts1} nerve terminals depleted by stimulation at elevated temperatures contain collared-pit structures, as shown in the inset of Figure 1*B*. Thus, stimulation of *shi*^{ts1} larval neuromuscular preparations with high-K^+ saline at elevated temperatures causes depletion of synaptic vesicles and the accumulation of collared pits on presynaptic membrane, as expected from the previous studies of adult synapses (Kosaka and Ikeda, 1983). Having established that an intermediate stage in synaptic vesicle recycling can be trapped at larval neuromuscular synapses, we proceeded to characterize the relative localization and redistribution of two components of *Drosophila* synaptic vesicle membrane in wild-type terminals as well as *shi*^{ts1} terminals depleted of synaptic vesicles.

Two synaptic vesicle proteins are identically redistributed in vesicle-depleted terminals

The best marker for *Drosophila* synaptic vesicles is synaptotagmin, an integral membrane protein shown to be associated with synaptic vesicles by biochemical, morphological, and genetic criteria (DiAntonio et al., 1993; Littleton et al., 1993; Ramaswami et al., 1994; van de Goor et al., 1995). Yet another potentially excellent marker for synaptic vesicles is the cysteine-string protein (csp), a heavily fatty-acylated, cysteine-rich component of synaptic vesicles that lacks a transmembrane domain (Mastrogiacomo et al., 1994; Zinsmaier et al., 1994). The best-characterized marker for presynaptic plasma membrane is a carbohydrate epitope fortuitously recognized by an anti-HRP antibody (Jan and Jan, 1982; Katz et al., 1988). Immunoelectron microscopy has been used to show that this epitope is highly enriched on insect neuronal cell surface (Sabry et al., 1991). In Western blots, the axonal protein most strongly labeled by anti-HRP is a membrane- and cytoskeleton-associated β subunit of the Na^+/K^+ ATPase (Sun and Salvaterra, 1995; van de Goor et al., 1995). We have shown previously by optical microscopy that the csp seems to redistribute in synaptic vesicle-depleted *shi*^{ts1} terminals from an intracellular compartment surrounded by anti-HRP immunoreactivity to a compartment indistinguishable from plasma membrane (Ramaswami et al., 1994; van de Goor et al., 1995).

To confirm that csp and synaptotagmin may be used interchangeably as morphological markers for synaptic vesicle membrane, we used confocal microscopy to assess systematically the relative distributions of synaptotagmin, csp, and anti-HRP in wild-type and *shi*^{ts1}-depleted Type 1b nerve terminals (see Materials and Methods). First, we examined *Drosophila* neuromuscular junctions double-stained for synaptotagmin and anti-HRP immunoreactivity. In wild-type synapses stimulated for 5 min at 34°C, the relative distribution of plasma membrane and synaptic vesicles was not altered significantly from resting

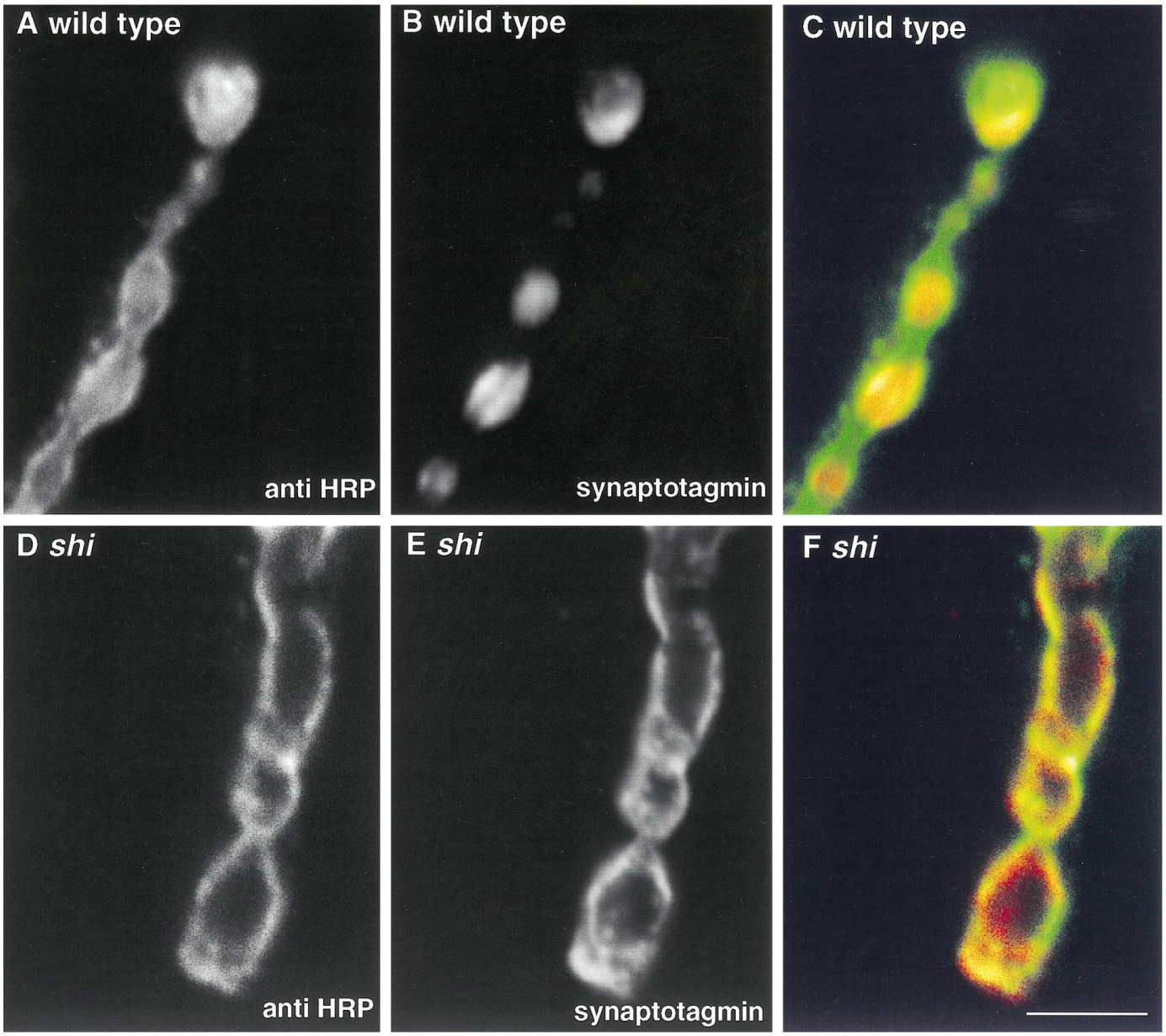

Figure 2. Synaptotagmin is redistributed from an intracellular pool to plasma membrane in *shi*^{ts1} mutant terminals. Each image represents a single optical section. *A–C*, Wild-type presynaptic terminals stimulated at elevated temperatures. *A*, Plasma membrane antigens labeled by anti-HRP. *B*, Synaptic vesicles labeled by anti-synaptotagmin. *C*, A red–green overlay of the two (green plasma membrane and red synaptic vesicles) shows that the synaptic vesicle marker synaptotagmin is restricted to presynaptic varicosities and surrounded by plasma membrane labeled by anti-HRP. *D–F*, In *shi*^{ts1} terminals depleted of synaptic vesicles, plasma membrane antigens (*D*) and synaptic vesicle antigens (*E*) show almost identical distribution patterns. The red–green overlay (*F*) indicates that synaptic vesicle membrane protein (*red*) is trapped on plasma membrane (*green*). Residual anti-HRP immunoreactivity apparently within wild-type varicosities is not seen in optical sections through *shi*^{ts1}-depleted nerve terminals. This phenomenon could reflect swelling of *shi*^{ts1} nerve terminals after substantial addition of synaptic vesicle membrane to the plasmalemma. Such swelling could result in a much higher efficiency of optical sectioning and improved resolution along the *Z*-axis between the inside of the bouton and the overlying plasma membrane. An alternative possibility we cannot exclude is that anti-HRP may additionally recognize an unidentified component of synaptic vesicle membrane. Scale bar (shown in *F*): 5 μm.

terminals: synaptic vesicles were in dense and compact structures specifically localized within presynaptic varicosities surrounded by plasma membrane (Fig. 2*A–C*). In vesicle-depleted *shi*^{ts1} nerve terminals, synaptotagmin is redistributed dramatically compared with wild-type or resting *shi* terminals. After synaptic vesicle depletion, synaptic vesicle membrane appears almost indistinguishable from plasma membrane by confocal microscopy (Fig. 2*D–F*).

After establishing that synaptotagmin redistributes to plasma membrane in *shi*^{ts1}-depleted larval motor terminals, we examined the relative distributions of synaptotagmin and csp. The images shown in Figure 3*A,B* compare synaptotagmin and csp localization within wild-type presynaptic varicosities, which have been stimulated with high-K^+ saline for 5 min at 34°C. Images in Figure 3*C,D* show an identically treated *shi*^{ts1} preparation. At the level of resolution afforded by light microscopy, the distributions of syn-

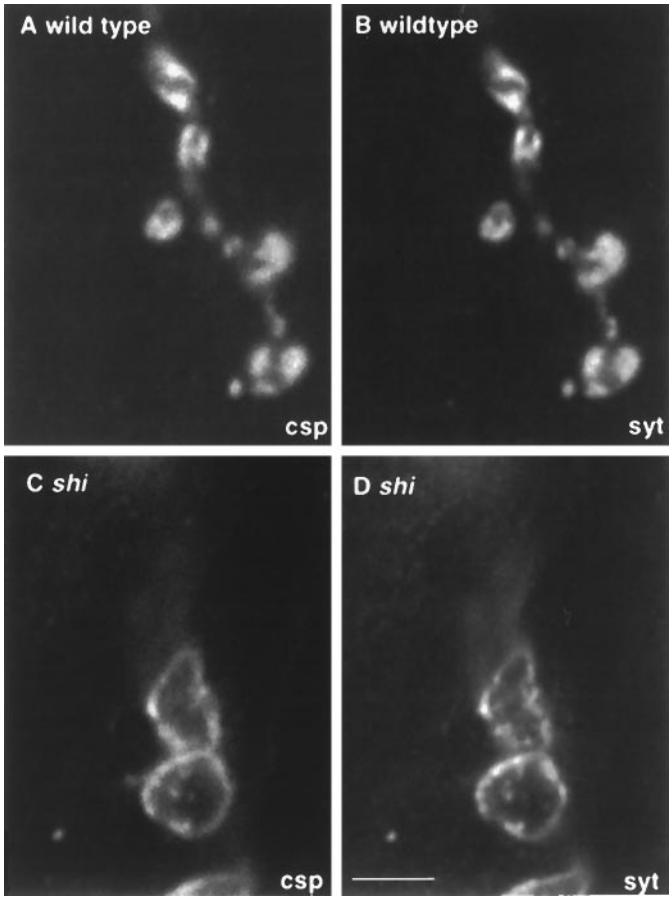

Figure 3. Synaptotagmin and cysteine string protein (*csp*) are identically localized within synaptic boutons. *A, B*, Single optical sections through wild-type terminals stimulated at 34°C, stained for *csp* (*A*) and synaptotagmin (*syt*) (*B*). Identical dense subsynaptic regions are labeled within presynaptic boutons. *C, D*, In similar sections through *shi*^{ts1}-depleted terminals, both *csp* (*C*) and *syt* (*D*) are redistributed to identical ring-shaped structures probably corresponding to plasma membrane. Scale bar (shown in *D*): 5 μm.

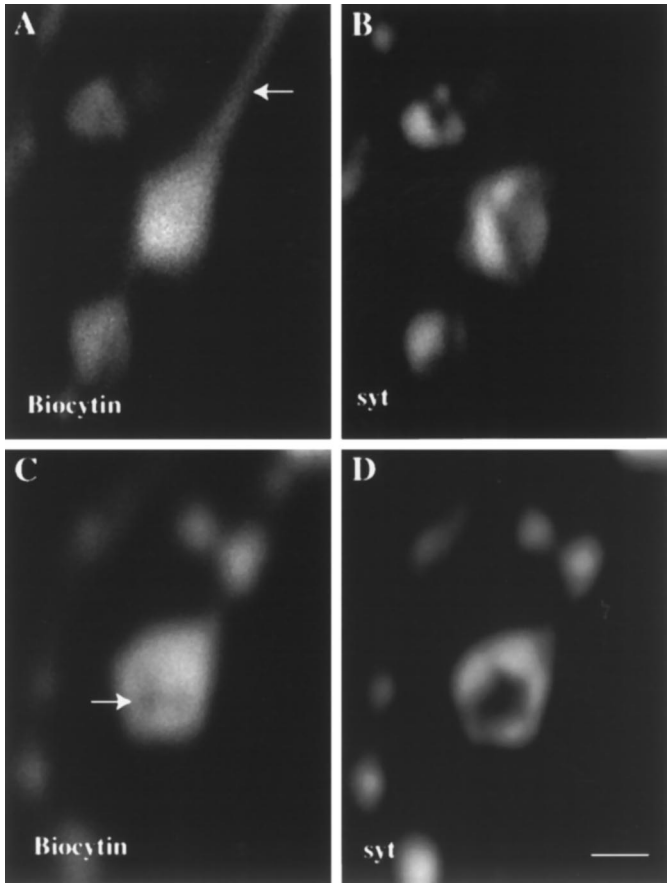

Figure 4. A small freely diffusible molecule has access to most of the nerve terminal. Wild-type presynaptic boutons were filled with biocytin (a small diffusible molecule), and the relative distributions of biocytin and synaptic vesicles are compared in the same optical sections. *A*, Biocytin is found in the axonal regions (marked by an *arrow*) connecting varicosities in addition to the entire varicosity itself. *B*, In the same sample shown in *A*, synaptic vesicles are found tightly localized to specific subsynaptic regions within individual varicosities. *C* and *D* show a different preparation from *A* and *B*. Here a small central region of the presynaptic bouton (indicated by an *arrow*), which does not contain synaptic vesicle marker (*D*), is relatively inaccessible to biocytin. The axonal region is not seen in this optical section. Scale bar, 2 μm.

aptotagmin and csp are indistinguishable within wild-type or vesicle-depleted presynaptic varicosities.

Our results establish that csp and synaptotagmin immunoreactivity can be used as reference points to mark synaptic vesicles within resting Type 1b larval nerve terminals. In *shi*^{ts1} terminals depleted of synaptic vesicles, csp and synaptotagmin may serve as good morphological markers for presynaptic plasma membrane. An additional observation we wish to underscore is that two synaptic vesicle antigens show *identical* distributions in our experimental system. This apparent absolute identity is an important point, because it serves to emphasize the differences we have subsequently observed between localizations of dynamin and synaptic vesicle markers.

Almost the entire mature nerve terminal is accessible to a small soluble molecule

The nerve terminal contains synaptic vesicle clusters, mitochondria, and various cytoskeletal elements in addition to soluble cytoplasmic material. Previous EM studies have shown that in *Drosophila*, frog, and mammals, synaptic vesicles do not occupy the entire motor nerve terminal. Optical microscopy has also been used to demonstrate synaptic vesicle subdomains at the frog and mammalian neuromuscular junction, which may be distinguished from domains rich in mitochondria (Lichtman et al., 1989; Betz et al., 1992; Atwood et al., 1993; Jia et al., 1993). To our knowledge, however, the distribution of a freely diffusible small molecule has never been imaged at high resolution within the nerve terminal. This is a significant issue because it is possible, for instance, that a large fraction of the presynaptic cytosol occupied by synaptic vesicle clusters and mitochondria remains relatively inaccessible to soluble cytoplasmic proteins. In this scenario, a small soluble molecule whose distribution is governed purely by diffusion into accessible regions of the presynaptic cytosol would appear enriched in subdomains of the presynaptic varicosity. To investigate this question, we filled Type 1b nerve terminals with biocytin, a charged, membrane-impermeant, soluble molecule, and examined its localization by confocal microscopy. Under conditions in which the distribution of synaptotagmin was qualitatively unchanged, biocytin appeared smoothly and almost uniformly distributed within the nerve terminal.

The relative distribution of biocytin and synaptotagmin in filled wild-type terminals is shown in Figure 4. The optical sections in Figure 4, *A* and *B*, show that biocytin can be easily visualized in

the axonal regions connecting presynaptic varicosities, whereas synaptotagmin is restricted to the varicosity itself. Although in these images biocytin appears to fill the entire bouton, in the images shown in Figure 4, *C* and *D*, there appears to be a small region within the varicosity relatively inaccessible to both biocytin and synaptic vesicles. It is possible that this biocytin-inaccessible region contains mitochondria, a hypothesis we have not tested in this study. Our major conclusion from the biocytin-fill experiments is that a freely diffusible molecule in nerve terminals must show two properties. (1) It must be found in the axonal tracts connecting presynaptic varicosities, and (2) it should appear smoothly distributed within a presynaptic varicosity, not in a patchy or punctate pattern.

Dynamin is restricted to synaptic varicosities in a pattern different from synaptotagmin

To compare the distribution of dynamin relative to our compartment-specific markers, we generated three independent antisera against *Drosophila* dynamin: shi-3 antibody was raised against a C-terminal peptide, and the antisera Ab2073 and Ab2074 were raised against bacterial fusion proteins containing different domains of fly dynamin (for more details, see Materials and Methods). In Western blots against proteins from fly head lysates, all three antibodies labeled a ~92/94 kDa doublet, the appropriate size for the *Drosophila* dynamin (Gass et al., in press) (Fig. 5*A*). When affinity-purified against a fusion protein including the complete dynamin protein, all three of the antisera recognized this protein exclusively. Unpurified shi-3 antiserum, affinity-purified 2073, and affinity-purified 2074 antisera strongly labeled both type 1b and type 1s presynaptic varicosities at the larval neuromuscular junction (Fig. 5*B*). Having established that the antibodies recognize a presynaptically concentrated *Drosophila* dynamin, we used them to localize dynamin at a fine level relative to other compartment-specific markers at the fly nerve terminal. Indistinguishable results were obtained with all three independent antisera.

In resting wild-type terminals, dynamin, like the synaptic vesicle marker csp, is localized within presynaptic varicosities and absent from axonal regions between the varicosities (Fig. 6*A–C*). Because this is not the distribution expected for a freely diffusible molecule like biocytin, we suggest that an active mechanism must exist to restrict its diffusion into axonal regions between synaptic sites. In higher-resolution images comparing dynamin localization with csp (Fig. 6*D–F*), dynamin has a patchy distribution, quite different from synaptic vesicles labeled by anti-csp. The differences in the observed localization patterns of dynamin, csp, and biocytin suggest that in resting terminals, dynamin occupies a region of the presynaptic terminal distinct from compartments labeled by biocytin and csp. This dynamin-rich domain is not likely to be a specialized region of presynaptic plasma membrane, because anti-HRP immunoreactivity surrounds the dynamin-containing regions of synaptic boutons (data not shown).

Although the distribution pattern of dynamin is distinct from that of synaptic vesicles, dynamin immunoreactive regions overlap spatially with synaptic vesicle-containing regions. In addition to synaptic vesicles, this region of the bouton is likely to contain a complex cytoskeletal matrix that is not easily revealed by conventional EM studies. One function of this presynaptic cytoskeleton is to hold synaptic vesicles close to synaptic sites (Rosahl et al., 1995). It is tempting to speculate that dynamin association with a component of this same cytoskeletal meshwork may serve to prevent its diffusion out of the presynaptic varicosities. Alternatively, dynamin may associate with several different presynaptic compartments in resting terminals, but this seems to be a less likely possibility (see Discussion).

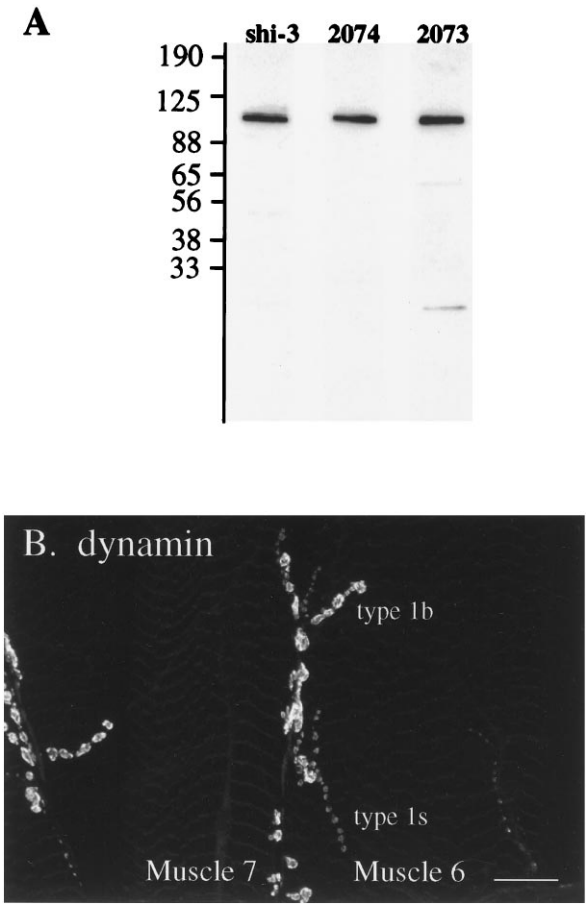

Figure 5. *A*, *Drosophila* dynamin antibodies shi-3 (whole anti-peptide serum), Ab2073, and Ab2074 (affinity-purified antibodies) label dynamin by Western blot analysis. Fifteen milligrams of *Drosophila* S1 postnuclear supernatant were resolved by SDS-PAGE, transferred to nitrocellulose, and incubated with the indicated antibody. Each antibody specifically labels dynamin, a 92/94 kDa doublet whose individual components are not resolved in this gel (Gass et al., in press). *B*, Each of the antisera stain type 1b and type 1s varicosities at the larval neuromuscular junction. This image shows a preparation stained with affinity-purified Ab2074. Thus, dynamin is highly enriched at the motor terminal, quite specifically at varicosities (see also Fig. 7). Scale bar, 25 μm.

In vesicle-depleted *shi*^{ts1} boutons, dynamin redistributes to plasma membrane subdomains

Previous biochemical experiments on mammalian synaptosomes have shown that an apparently soluble pool of dynamin is mobilized rapidly to a membrane-bound pool by synaptosome stimulation (Robinson et al., 1994). These biochemical experiments were supported and extended by beautiful immuno-EM studies demonstrating the association of dynamin with nascent endocytotic structures on plasma membranes of perforated synaptosomes treated with GTPγS (Takei et al., 1995). For these reasons, we expected to find dynamin redistributed to plasma membrane in *shi*^{ts1}-depleted nerve terminals (see Discussion). To investigate this issue, we depleted *shi*^{ts1} nerve terminals of synaptic vesicles by stimulation at elevated temperatures and used the antibodies shi-3, Ab2073, and Ab2074 to examine the potential redistribution

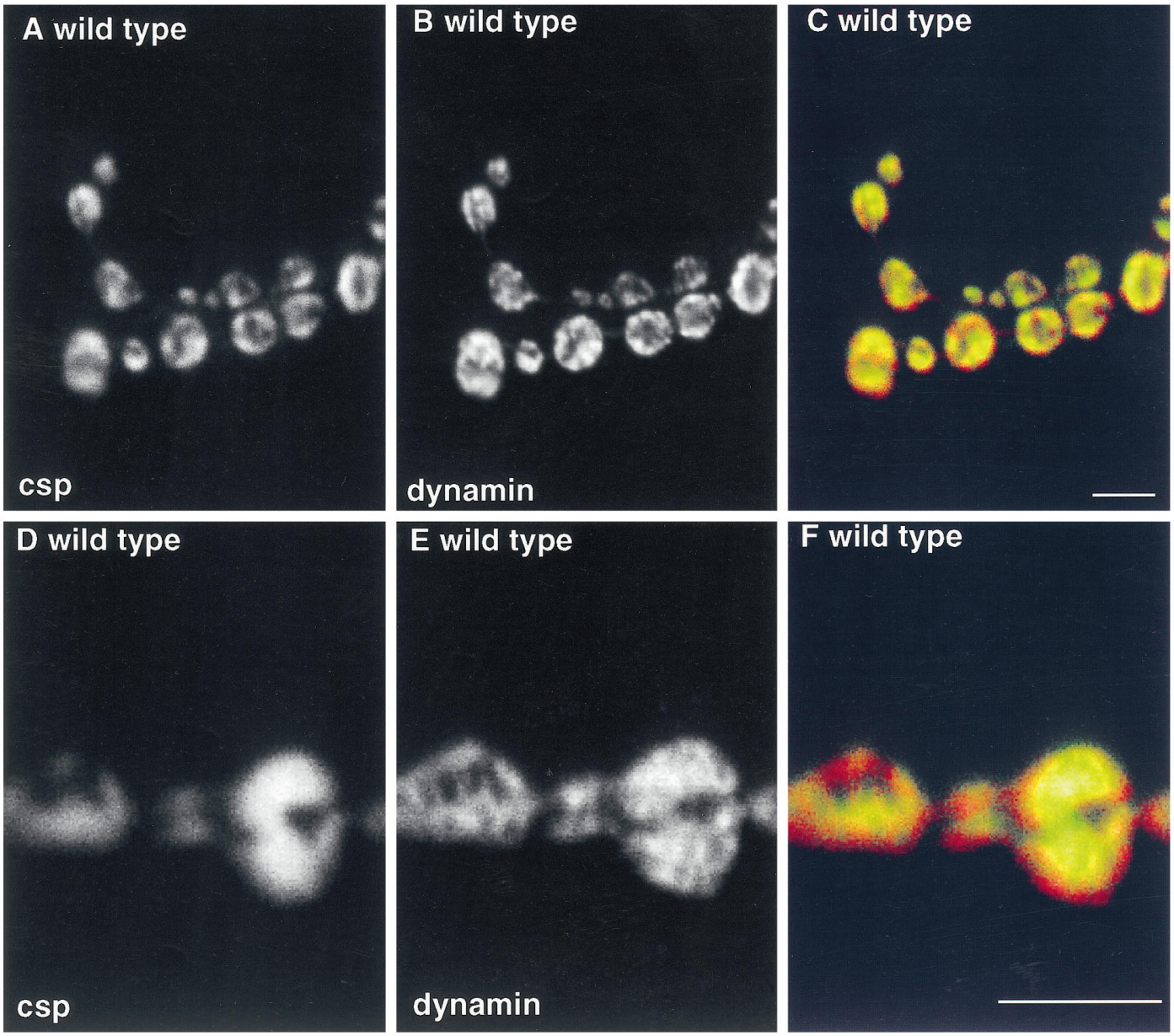

Figure 6. Dynamin is localized in presynaptic varicosities to subdomains that do not correspond to synaptic vesicles. *A–C*, Lower-resolution images of resting wild-type 1b boutons labeled with anti-dynamin (*B*), anti-csp (*A*), and a red (*dynamin*)–green (*csp*) overlay of the two images (*C*) show that like synaptic vesicles, dynamin is restricted to presynaptic varicosities. *D–F*, Higher-resolution images showing that dynamin (*E*) has a different distribution from synaptic vesicles (*D*) within individual boutons. This is emphasized in the red–green overlay (*F*). Note in Figure 4, *A* and *B*, the identity between csp and synaptotagmin localization in a similar preparation. Single optical sections. Scale bar, 5 μm.

of dynamin. All three antibodies, independently used, gave us similar results.

In *shi*^{ts1}-depleted type 1b presynaptic varicosities, almost all of the synaptic vesicle marker csp redistributes to plasma membrane (Figs. 3, 7*A,D*). This distribution of csp on the plasmalemma is relatively smooth. Under similar conditions, dynamin, like csp, is redistributed to the plasma membrane, and little residual cytoplasmic dynamin can be seen within the bouton (Fig. 7*B,E*). Unlike csp, however, dynamin immunoreactivity shows a strikingly punctate distribution. It is tightly concentrated in specific regions of the plasma membrane that are not necessarily enriched in the synaptic vesicle marker (see *arrows* in Fig. 7*B,E*). The functional implication of these dynamin hot spots is considered in the Discussion.

DISCUSSION

Compartment-specific markers for the *Drosophila* larval motor terminal

Immunofluorescence microscopy has become an increasingly powerful tool for the study of cellular structure and membrane traffic. The most valuable feature of this technique is that it enables direct observation of the relative distributions of as many as three different antigens at a whole-cell level, to 300 nm resolution. Thus, it allows comparison of the distributions of an unknown antigen relative to one or more "markers" that serve as reference points. One concern in the interpretation of immunofluorescence images is the innate complexity of eukaryotic cells. For instance, different Golgi compartments, Golgi-

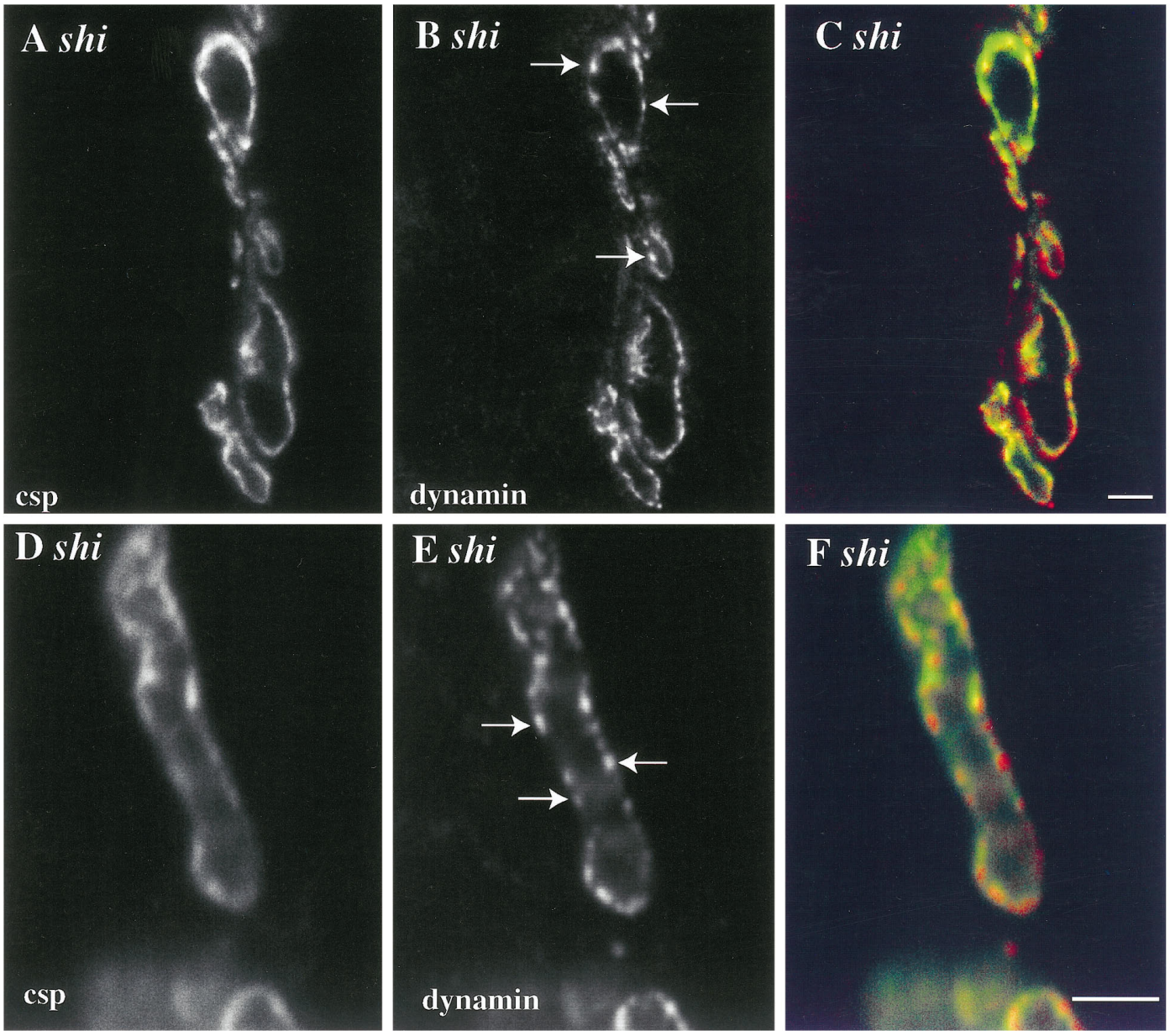

Figure 7. Dynamin is redistributed to hot spots on the plasma membrane in *shi*^{ts1}-depleted terminals. Synaptic vesicle proteins (*A*, *D*) are redistributed to the plasma membrane in a pattern that is smooth, relative to the punctate distribution of dynamin (*B, E*). The red–green overlays in *C* and *F* emphasize these differences. The *arrows* in *B* and *E* indicate dynamin-rich domains not particularly enriched in the synaptic vesicle marker. Single optical sections. Scale bar, 5 μm.

associated vesicles, and various endosomal structures are not necessarily distinguishable by optical microscopy. Not only can marker specificity be a problem in a naturally dynamic cell, but different structures labeled by the marker may be very closely associated (Griffiths et al., 1993). Despite these caveats, however, immunofluorescence microscopy has been used successfully to study subcellular architecture and dynamics in yeast cells not much more than 5μm in size (Adams and Pringle, 1984; Kilmartin and Adams, 1984).

Single presynaptic varicosities at the *Drosophila* larval neuromuscular junction may be the same size as yeast cells. The relatively few cellular structures found at nerve terminals may also allow less ambiguous identification of labeled structures viewed under the light microscope. For these reasons, immunofluorescence microscopy promises to be an important and useful tool for studying membrane dynamics at these nerve terminals. The availability of genetic mutants, functional assays for synaptic transmission, and a large collection of identified presynaptic molecules form an especially attractive context for such analyses in *Drosophila*. Some recent studies have begun to exploit the convenience of *Drosophila* motor terminals for high-resolution optical microscopy (Kurdyak et al., 1994; Lahey et al., 1994; Ramaswami et al., 1994; Bate and Broadie, 1995; van de Goor et al., 1995). Our results presented here, however, constitute the first systematic attempt to characterize molecular markers specific for each major compartment of the presynaptic terminal. We summarize below the

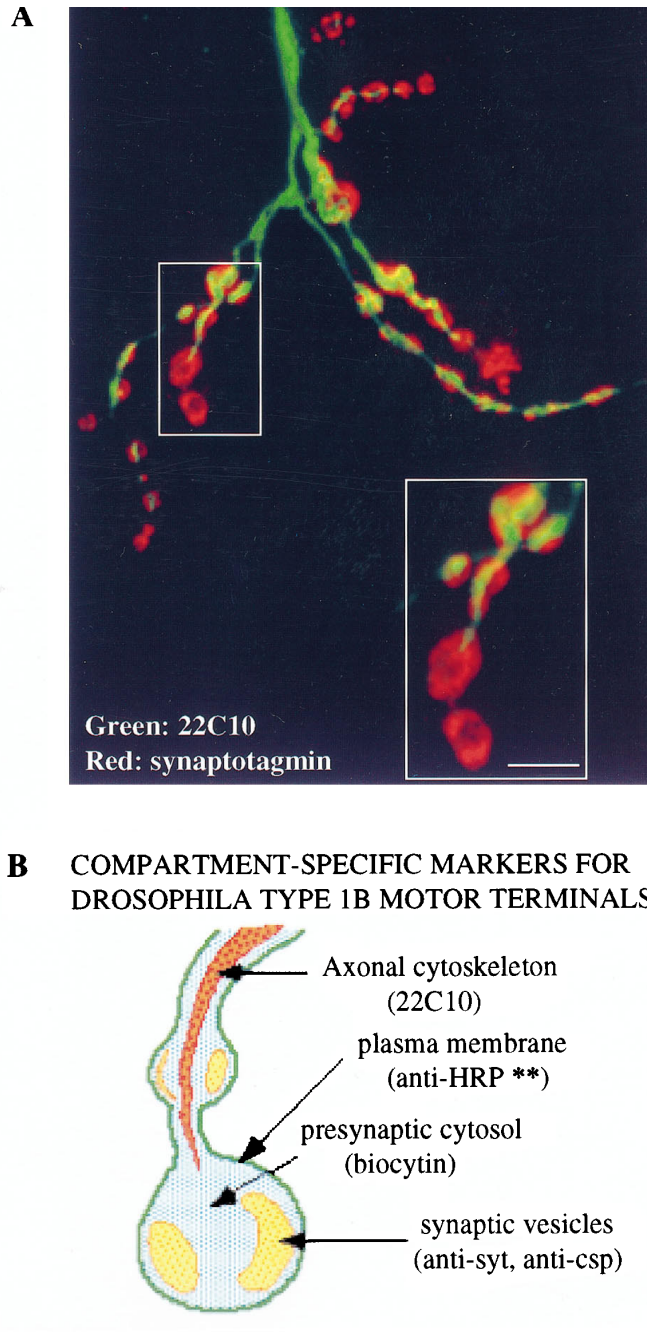

Figure 8. *A*, The monoclonal antibody 22C10 labels a component of the axonal cytoskeleton. Scale bar, 5 μm. *B*, A cartoon showing various compartment-specific markers in type 1b presynaptic boutons. **Our data do not exclude the possibility that anti-HRP recognizes a component of synaptic vesicle membrane in addition to the presynaptic plasma membrane. An additional marker not characterized in our study is 4-di-2-Asp, which labels mitochondria (Magrassi et al., 1987; Kurdyak et al., 1994).

validity and distribution patterns of candidate markers for (1) synaptic vesicles, (2) plasma membrane, (3) cytoplasm, (4) mitochondria, (5) a microtubule-based axonal cytoskeleton, and (6) a presynaptic cytomatrix (Fig. 8*B*).

Synaptic vesicles, plasma membrane, and presynaptic cytosol

The images shown in Figures 2, 3, and 4 indicate that synaptic vesicles labeled by either anti-csp antibody or anti-synaptotagmin antibody are localized spatially in a pattern clearly distinguishable from plasma membrane stained by the anti-HRP antibody and presynaptic cytosol labeled by intracellular fills of biocytin. The appropriateness of anti-csp and DSYT-2 antibodies to mark *Drosophila* synaptic vesicles and of anti-HRP antibodies to mark presynaptic plasma membrane have been discussed here and in an earlier report (van de Goor et al., 1995). This is the first reported use of biocytin fills to mark presynaptic cytosol at motor terminals. Although immuno-EM studies are lacking, we suggest that biocytin is an excellent marker for small, freely diffusible molecules at the nerve terminal. Biocytin is a very soluble, charged molecule that does not cross a lipid bilayer. It diffuses passively down axons and carries an amino-modification (on biotin), which allows convenient fixation and visualization by streptavidin-conjugated probes. Its localization pattern, shown in Figure 4, indicates that most of the cytosol within presynaptic varicosities and between the varicosities remains freely accessible to such soluble molecules.

Mitochondria

We have not characterized the distribution of mitochondria in this paper, but previous work has shown that the vital dyes Rhodamine 123 and 4-Di-2-Asp may be used to specifically label presynaptic mitochondria in a wide range of species, including *Drosophila* (Yoshikami and Okun, 1984; Magrassi et al., 1987; Atwood et al., 1993; Broadie and Bate, 1993; Kurdyak et al., 1994). EM studies of *Drosophila* nerve terminals suggest that Type 1b boutons contain high concentrations of mitochondria, which because of their large size could exclude synaptic vesicles from regions they occupy (Atwood et al., 1993).

The axonal cytoskeleton

We suggest here that the monoclonal antibody 22C10, commonly used to mark neuronal projections in *Drosophila*, may specifically label the axonal cytoskeleton. The antibody labels a unique compartment within axons and synaptic boutons quite different from any of the other markers we have examined (Fig. 8). 22C10 immunoreactivity runs like a wire down the middle of the axon and does not invade regions of the presynaptic varicosities occupied by synaptic vesicles. Although previous low-resolution studies have suggested that 22C10 may mark a neuronal cell surface integral membrane protein (Goodman et al., 1984; Schulze et al., 1995), our data show that 22C10 marks an intracellular axonal compartment at *Drosophila* nerve terminals, which is surrounded by plasma membrane marked with anti-HRP (Fig. 8) (our unpublished data). 22C10 staining at nerve terminals is clearly *not* associated with neuronal plasma membrane. These data are consistent with published observations that 22C10 staining labels axonal processes but not presynaptic varicosities (Keshishian et al., 1993). Which specific component of the axonal cytoskeleton is labeled by 22C10 remains to be seen.

Potential uses

With some caveats mentioned above, good molecular markers seem to exist for all known major compartments at *Drosophila* type 1b nerve terminals (Fig. 8*B*), except the complex presynaptic cytomatrix, which is most apparent in rapidly frozen, deep-etched preparations viewed under the electron microscope (Landis et al., 1988; Hirokawa et al., 1989). The existence of such compartment-specific markers within large presynaptic varicosities allows the use of the most attractive features of immunofluorescence microscopy to study subcellular architecture and dynamics within *Drosophila* motor terminals. Our studies of dynamin localization

within wild-type and *shi*^{ts1} presynaptic terminals derive from this characterization of compartment-specific markers. These may serve as a model for future fine analyses of new and currently known presynaptic proteins by optical microscopy.

Localization of dynamin in resting nerve terminals

This is the first report to show a concentration of dynamin at neuromuscular synapses. Our data show that dynamin is localized not only to synaptic sites at motor terminals but is also found in a distribution different from all compartment-specific markers that we have analyzed. We consider the relevance of these observations in the light of current knowledge of nerve-terminal architecture and dynamin function.

Dynamin is restricted to synaptic sites

In resting *Drosophila* motor terminals, dynamin is localized to synaptic varicosities. This observation suggests the existence of a mechanism to restrict free diffusion of presynaptic dynamin.

The state of dynamin in resting nerve terminals from mammalian brain has been examined by biochemical methods (for review, see Robinson et al., 1994). Dynamin isolated from lysed unstimulated synaptosomes seems to be a soluble phosphoprotein, whereas dynamin from briefly stimulated synaptosomes is predominantly dephosphorylated and associated with plasma membrane. Although these biochemical experiments suggest dynamin to be in a soluble state in resting nerve terminals, it remains possible that interactions between dynamin and specific presynaptic components are disrupted during homogenization of synaptosomes. Immunofluorescence localization of dynamin in primary neuronal cultures from rat hippocampus suggests that dynamin is not restricted, like synaptic vesicle membrane proteins, to specific synaptic sites in these cultured CNS neurons (McPherson et al., 1994b; David et al., 1996). To reconcile these observations with our data, we suggest that mechanisms required for restricting the distribution of dynamin within the nerve terminal cytosol are less well developed in synapses among cultured hippocampal neurons than at *Drosophila* motor terminals. If the number of dynamin-binding sites were limited in cultured hippocampal synapses, then excess dynamin could diffuse freely within the axon. Significantly, overexpression of dynamin in HeLa cells results in an accumulation of soluble cytoplasmic dynamin (Damke et al., 1994). In any event, our results show unambiguously that dynamin at fly motor terminals is restricted to presynaptic varicosities, not freely diffusible like biocytin. Our higher resolution images suggest a possible mechanism for retention of dynamin at these synaptic sites.

Dynamin may associate with a presynaptic cytoskeleton

Because synapses in primary hippocampal cultures are very small in size, optical microscopy has not been used to obtain fine-resolution images for dynamin localization within individual synaptic sites. Our results show that within individual *Drosophila* presynaptic boutons, dynamin is localized in the same approximate region as synaptic vesicles but in a clearly distinct pattern. One possibility is that dynamin is distributed in a complex manner among different presynaptic compartments. A more attractive possibility is that dynamin in resting synapses is associated with a specific presynaptic compartment not characterized in our study. What might such a compartment be?

A vast body of EM studies has shown that this region of the presynaptic terminal in all species examined contains relatively few cellular structures. These include endosomes and dense-core vesicles, but predominantly presynaptic cytosol, synaptic vesicles, and a cytoskeletal meshwork not easily visualized by conventional EM studies (Burns and Augustine, 1995). Resting type 1b nerve terminals contain few, if any, endosomes or dense-core granules (Atwood et al., 1993; Jia et al., 1993). The patchy distribution pattern of dynamin is quite different from the observed distribution of presynaptic cytosol (labeled by biocytin) or synaptic vesicles. Thus, dynamin is possibly associated with a component of the tangled, uncharacterized cytoskeletal meshwork that lies within this region of the nerve terminal. Immuno-gold EM may not be a useful way to investigate this hypothesis, because elements of the cytomatrix have been clearly defined only in rapidly frozen, deep-etched preparations and are not easily visualized under conventional EM studies. Proposed structural components of this cytomatrix include actin, fodrin, and myosin (Landis et al., 1988; Bernstein and Bamburg, 1989; Hirokawa et al., 1989; Mochida et al., 1994; Burns and Augustine, 1995).

At least one synapse-specific protein, synapsin, is known to interact with this cytomatrix (Ceccaldi et al., 1995). There are several compelling similarities emerging between synapsin and dynamin (McPherson et al., 1994a; De Camilli et al., 1995; Morris and Schmid, 1995). Like dynamin in *Drosophila* motor terminals, synapsin at frog motor terminals is restricted to synaptic sites and does not distribute evenly in the accessible presynaptic cytosol (Torri-Tarelli et al., 1992). This localization may require association of synapsin with presynaptic cytoskeletal elements via its C-terminal proline-rich sequences. Similar C-terminal proline-rich domains in dynamin may interact with a component of the same cytomatrix to restrict dynamin diffusion. Associations mediated by proline-rich domains of both proteins are probably regulated by phosphorylation, and both seem to redistribute after nerve stimulation (Torri-Tarelli et al., 1992; McPherson et al., 1994a; De Camilli et al., 1995). Because synapsin homologs have not yet been reported in *Drosophila*, at present we cannot examine the relative distributions of dynamin and synapsin.

Redistribution of dynamin in *shi*^{ts1} mutants

A specific intermediate stage in synaptic vesicle recycling is trapped in shi^{ts1} *mutants*

Dynamin may undergo a series of transitions while participating in sequential membrane rearrangements during the different stages of vesicle internalization (Morris and Schmid, 1995; De Camilli et al., 1995). Several lines of evidence suggest that in *shi*^{ts1} mutant synapses at elevated temperatures, dynamin is unable to undergo a specific transition that requires GTP hydrolysis by membrane-associated dynamin (Damke et al., 1995).

In perforated synaptosomes incubated with GTPγS, conditions in which all presynaptic GTPases are expected to be in their GTP-bound state, dynamin is found associated with an exaggerated neck of nascent endocytotic vesicles (Takei et al., 1995). Because the dynamin-containing structures on these vesicle necks are of the same size and disposition as the "collars" in collared pits trapped in *shi*^{ts1} mutant synapses, it is likely that in both GTPγS-treated and *shi*^{ts1} mutant synapses, GTPase activity is similarly inhibited (Kosaka and Ikeda, 1983) (Fig. 2). This hypothesis is supported further by the molecular lesion associated with *shi*^{ts1}. The *shi*^{ts1} mutation alters a single amino acid (Gly 267-Tyr) in the GTPase domain of dynamin, some distance from the predicted GTP-binding regions (van der Bliek and Meyerowitz, 1991). Similar substitutions in the homologous yeast GTPase

VPS1, which cause dominant negative phenotypes like *shi*^{ts1}, do not generally affect GTP binding but may affect GTP hydrolysis instead (Vater et al., 1992). Thus, we suggest that at elevated temperatures, both dynamin and recycling synaptic vesicles in *shi*^{ts1} synapses are trapped at a specific stage requiring GTP hydrolysis by dynamin. At this stage, synaptic vesicle membrane protein is found distributed relatively smoothly over the plasmalemma when compared to the far more punctate pattern of dynamin localization on the presynaptic plasma membrane.

Redistribution of dynamin to plasma membrane in shi^{ts1}*-depleted terminals*

Our observation that an intracellular pool of dynamin in resting synapses is redistributed in *shi*^{ts1} mutants is consistent with biochemical studies on mammalian synaptosomes but contrasts with biochemical studies of dynamin from whole *Drosophila* head homogenates (Robinson et al., 1994; Gass et al., in press). The most economical explanation for this discrepancy is that dynamin at synapses and in other cellular contexts shows different biochemical properties. In this discussion we consider the traffic of dynamin only at presynaptic terminals.

In *shi*^{ts1} larval nerve terminals stimulated at elevated temperatures, dynamin is dramatically redistributed to plasma membrane. Under these conditions, intracellular dynamin is reduced to a level too low for detection by our immunofluorescence technique. This almost quantitative redistribution of dynamin must be discussed in the context of a mutant nerve terminal in a nonphysiological state.

The total surface area of synaptic vesicle membrane in resting terminals may exceed the area of presynaptic plasma membrane (Koenig and Ikeda, 1989). Thus, in *shi*^{ts1} terminals drastically depleted of synaptic vesicles, the endocytotic cargo (synaptic vesicle membrane proteins) on the plasma membrane has been increased enormously. It is likely that most of the endocytotic machinery has been saturated under these conditions. This hypothesis is supported by two experimental observations. (1) In adult *shi*^{ts1}-depleted synapses, the surface area of observed collared pits is only a small fraction of the total surface area of depleted synaptic vesicles (Kosaka and Ikeda, 1983), and (2) our immunofluorescence images of *shi*^{ts1}-depleted terminals show that a large fraction of synaptic vesicle membrane protein is found in regions not enriched for dynamin, an essential component of the endocytotic machinery.

What may be the mechanism of the observed redistribution of dynamin? Biochemical observations of mammalian synaptosomes suggest that calcium entry after membrane depolarization results in calcium-dependent dephosphorylation of dynamin. Dephosphorylated dynamin is predominantly membrane-associated, whereas phospho-dynamin is found in the soluble fraction of homogenized synaptosomes. Both dephosphorylation and membrane association of dynamin seem to be inhibited by cyclosporine, an inhibitor of the calcium-dependent phosphatase calcineurin (Robinson et al., 1994). Although the details of this model remain to be demonstrated *in vivo*, it seems clear that dynamin associates with different proteins in resting terminals than in stimulated terminals; its transition from one set of partners to another is regulated by stimulation.

Dynamin hot spots on the plasma membrane

Although we anticipated a redistribution of dynamin to plasma membrane in *shi*^{ts1}-depleted terminals, the observation that dynamin was enriched at specific hot spots on the membrane was entirely unexpected. Because three independent antibodies against different domains of dynamin gave qualitatively identical results, the observed pattern of dynamin localization is not likely to be artifactual. Thus, in *shi*^{ts1}-depleted nerve terminals, subdomains of plasma membrane exist that are enriched for at least one component of the endocytotic machinery. We do not yet know how these hot spots are located relative to electron-dense bodies that mark active zones for synaptic vesicle exocytosis. It is worth noting that the subsynaptic distribution of clathrin, clathrin-associated proteins, and other likely components of the endocytotic machinery are unknown at this level of resolution. Our observations suggest that other molecules involved in synaptic vesicle endocytosis will be found enriched in these dynamin hot spots at *shi*^{ts1}-depleted nerve terminals.

The existence of dynamin "hot spots" suggests that dynamin-containing collared-pit structures are enriched in specific regions of the presynaptic plasma membrane. How might such hot spots arise, and what might be their functional relevance? We suggest two models: one, that they are generated in a temporal fashion made evident in *shi*^{ts1} synapses, and two, that they mark specialized zones for synaptic vesicle endocytosis. In model 1, we propose that membrane proteins from the first synaptic vesicles to fuse are trapped in collared pits. Because of obvious structural constraints, collared-pit structures may diffuse very slowly in the plane of the membrane. Once the available endocytotic machinery has been depleted, membrane proteins from still-fusing synaptic vesicles diffuse freely in the presynaptic plasma membrane away from the regions containing collared pits. (If one assumes a diffusion coefficient $D = 2 \times 10^{-10}$ cm^2/sec, a synaptic vesicle membrane protein is capable of diffusing up to 45 μm within the 5 min period of high-K^+ stimulation). In this first model, the spatial distribution of dynamin hot spots is controlled by the spatial distribution of synaptic vesicle fusion sites and the low rate of diffusion of collared-pit structures.

The second model derives from classical freeze-fracture studies of the frog neuromuscular synapse (Heuser and Reese, 1973, 1981). After synaptic vesicle exocytosis at active zones, large membrane particles corresponding to synaptic vesicle membrane proteins moved toward specific regions of the plasmalemma before membrane internalization. These active zones for synaptic vesicle endocytosis lie ~1 μm away from the fusion site, close to the regions where the presynaptic plasmalemma contacts Schwann cell processes (Heuser and Reese, 1973, 1981).

Although no Schwann cell-like processes have been described at the *Drosophila* neuromuscular junction, active zones for membrane retrieval may exist nevertheless. Specialized sites for endocytosis spatially distinct from fusion sites may serve an important cellular function. Unless synaptic vesicle membrane proteins are cleared away rapidly, the addition of synaptic vesicle membrane proteins would alter the biochemical composition of fusion sites and hence the efficiency of subsequent fusion events. Distinct zones for endocytosis may permit continuous transmitter release to occur with only marginal loss of efficiency due to alterations in presynaptic plasma membrane. Thus, in our second model, dynamin hot spots correspond to the spatially distinct active zones for synaptic vesicle endocytosis that have not been revealed previously by molecular markers.

Note added in proof: A paper describing *Drosophila* synapsins has been published since this manuscript was submitted: Klagges BRE, Heimbeck G, Godenschwege TA, Hofbauer A, Pflugfelder GO, Reifegerste R, Reisch D, Schaupp M, Buchner S, Buchner E

(1996) Invertebrate synapsins: a single gene codes for several isoforms in *Drosophila*.

REFERENCES

Adams AEM, Pringle JR (1984) Relationship of actin and tubulin distribution to bud growth in wild-type and morphogenetic-mutant *Saccharomyces cerevesiae*. J Cell Biol 98:934–945.

Atwood HL, Govind CK, Wu C-F (1993) Differential ultrastructure of synaptic terminals on ventral longitudinal abdominal muscles in *Drosophila* larvae. J Neurobiol 24:1008–1024.

Auld V, Fetter R, Broadie K, Goodman C (1995) Gliotactin, a novel transmembrane protein on peripheral glia, is required to form the blood-nerve barrier in *Drosophila*. Cell 81:757–767.

Bate CM (1993) The mesoderm and its derivatives. In: The development of *Drosophila* melanogaster (Bate CM, Martinez-Arias A, eds), pp 1013–1090. Cold Spring Harbor, NY: Cold Spring Harbor Laboratory.

Bate M, Broadie K (1995) Wiring the fly: the neuromuscular system of the *Drosophila* embryo. Neuron 15:513–525.

Bennett MK, Scheller RH (1993) The molecular mechanism of secretion is conserved from yeast to neurons. Proc Natl Acad Sci USA 90:2559–2563.

Bernstein BW, Bamburg JR (1989) Cycling of actin assembly in synaptosomes and neurotransmitter release. Neuron 3:257–265.

Betz WJ, Wu L-G (1995) Kinetics of synaptic-vesicle recycling. Curr Biol 5:1098–1101.

Betz WJ, Mao FM, Bewick GS (1992) Activity-dependent fluorescent staining and destaining of living vertebrate motor nerve terminals. J Neurosci 12:363–375.

Broadie KS, Bate M (1993) Development of the embryonic neuromuscular synapse of *Drosophila* melanogaster. J Neurosci 13:144–166.

Burns M, Augustine G (1995) Synaptic structure and function: dynamic organization yields architectural precision. Cell 83:187–194.

Ceccaldi PE, Grohovaz F, Benfenati F, Chieregatti E, Greengard P, Valtorta F (1995) Dephosphorylated synapsin I anchors synaptic vesicles to actin cytoskeleton: an analysis by video microscopy. J Cell Biol 128:905–912.

Chen YS, Obar RA, Schroeder CC, Austin TW, Poodry CA, Wadsworth SC, Vallee RB (1991) Multiple forms of dynamin are encoded by the shibire, a *Drosophila* gene involved in endocytosis. Nature 351:583–586.

Damke H, Baba T, Warnock DE, Schmid SL (1994) Induction of mutant dynamin specifically blocks endocytic coated vesicle formation. J Cell Biol 127:915–934.

Damke H, Baba T, van der Bliek A, Schmid S (1995) Clathrin-independent pinocytosis is induced in cells overexpressing a temperature-sensitive mutant of dynamin. J Cell Biol 131:69–80.

David C, McPherson P, Mundigl O, DeCamilli (1996) A role for amphiphysin in synaptic vesicle endocytosis supported by its binding to dynamin in nerve terminals. Proc Natl Acad Sci USA 93:331–335.

De Camilli P, Takei K, McPherson P (1995) The function of dynamin in endocytosis. Curr Opin Neurobiol 5:559–565.

DiAntonio A, Parfitt K, Schwarz TL (1993) Synaptic transmission persists in synaptotagmin mutants of *Drosophila*. Cell 73:1281–1290.

Garcia EP, McPherson PS, Chilcote TJ, Takei K, DeCamilli P (1995) rbSec1A and B colocalize with syntaxin 1 and SNAP-25 throughout the axon but are not in a stable complex with syntaxin. J Cell Biol 129:105–120.

Gass GV, Lin JJ-C, Scaife R, Wu C-F (1995) Two isoforms of *Drosophila* dynamin in wild-type and shibire ts neural tissue: different subcellular localization and association. J Neurogenet, in press.

Goodman CS, Bastiani M, Doe C, du Lac D, Helfand S, Kuwada J, Thomas JB (1984) Cell recognition during neuronal development. Science 225:1271–1279.

Grieco F, Hay JM, Hull R (1992) An improved procedure for the purification of protein fused with glutathione-*S*-transferase. Biotechniques 13:856–857.

Griffiths G, Parton RG, Lucocq J, van Deurs B, Brown D, Slot JW, Geuze HJ (1993) The immunofluorescent era of membrane traffic. Trends Cell Biol 3:214–219.

Heuser J, Reese T (1973) Evidence for recycling of synaptic vesicles during transmitter release at the frog neuromuscular junction. J Cell Biol 57:315–344.

Heuser J, Reese T (1981) Structural changes after transmitter release at the frog neuromuscular junction. J Cell Biol 88:564–580.

Hirokawa N, Sobue K, Kanda K, Harada A, Yorifuji H (1989) The cytoskeletal architecture of the presynaptic terminals and molecular structure of synapsin I. J Cell Biol 108:111–126.

Jan LY, Jan YN (1976) Properties of the larval neuromuscular junction in *Drosophila* melanogaster. J Physiol (Lond) 262:189–214.

Jan LY, Jan YN (1982) Antibodies to horseradish peroxidase as specific neuronal markers in *Drosophila* and in grasshopper embryos. Proc Natl. Acad Sci USA 79:2700–2704.

Jia X-X, Gorczyca M, Budnik V (1993) Ultrastructure of neuromuscular junctions in *Drosophila*: comparison of wild-type and mutants with increased excitability. J Neurobiol 24:1025–1044.

Johansen J, Halpern ME, Johansen KM, Keshishian H (1989) Stereotypic morphology of glutamatergic synapses on identified muscle cells of *Drosophila* larvae. J Neurosci 9:710–725.

Katz F, Moats W, Jan YN (1988) A carbohydrate epitope expressed uniquely on the cell surface of *Drosophila* neurons is altered in the mutant nac (neurally altered carbohydrate). EMBO J 7:3471–3477.

Keshishian H, Chiba A, Chang TN, Halfon MS, Harkins EW, Jarecki J, Wang L, Anderson M, Cash S, Halpern ME, Johansen J (1993) Cellular mechanisms governing synaptic development in *Drosophila* melanogaster. J Neurobiol 24:757–787.

Kilmartin J, Adams AEM (1984) Structural rearrangements of tubulin and actin during the cell cycle of the yeast *Saccaromyces*. J Cell Biol 98:922–933.

Koenig J, Ikeda K (1989) Disappearance and reappearance of synaptic vesicle membrane upon transmitter release observed under reversible blockage of membrane retrieval. J Neurosci 9:3844–3860.

Koenig J, Kosaka T, Ikeda K (1989) The relationship between the number of synaptic vesicles and the amount of neurotransmitter released. J Neurosci 9:1937–1942.

Kosaka T, Ikeda K (1983) Possible temperature-dependent blockage of synaptic vesicle recycling induced by a single gene mutation in *Drosophila*. J Neurobiol 14:207–225.

Kurdyak P, Atwood HL, Stewart BA, Wu C-F (1994) Differential physiology and morphology of motor axons to ventral longitudinal muscles in larval *Drosophila*. J Comp Neurol 350:463–472.

Lahey T, Gorczyca M, Jia X-X, Budnik V (1994) The *Drosophila* tumor suppressor gene *dlg* is required for normal synaptic bouton structure. Neuron 13:823–835.

Landis D, Hall A, Weinstein L, Reese T (1988) The organization of cytoplasm at the presynaptic active zone of a central nervous system synapse. Neuron 1:201–209.

Lichtman JW, Sunderland WJ, Wilkinson RS (1989) High resolution imaging of synaptic structure with a simple confocal microscope. New Biol 1:75–82.

Littleton TJ, Stern M, Schulze K, Perin M, Bellen HJ (1993) Mutational analysis of *Drosophila* synaptotagmin demonstrates its essential role in Ca^{2+}-activated neurotransmitter release. Cell 74:1125–1134.

Magrassi L, Purves D, Lichtman JW (1987) Fluorescent probes that stain living nerve terminals. J Neurosci 7:1207–1214.

Mastrogiacomo A, Parsons S, Zampighi G, Jenden D, Umbach J, Gunderson C (1994) Cysteine string proteins: a potential link between synaptic vesicles and presynaptic calcium channels. Science 263: 981–982.

McPherson PS, Czernik AJ, Chilcote TJ, Onofri F, Benfenati F, Greengard P, Schlessinger J, De Camilli P (1994a) Interaction of Grb2 via its Src homology 3 domain with synaptic proteins including synapsin I. Proc Natl Acad Sci USA 91:6486–6490.

McPherson PS, Takei K, Schmid S, De Camilli P (1994b) p145, a major Grb2-binding protein in brain is colocalized with dynamin in nerve terminals where it undergoes activity-dependent dephosphorylation. J Biol Chem 269:30132–30139.

Mochida S, Kobayahi H, Matsuda Y, Yuda Y, Muramoto K, Nonomura Y (1994) Myosin II is involved in transmitter release at synapses formed between rat sympathetic neurons in culture. Neuron 13:1131–1142.

Morris SA, Schmid SL (1995) The ferrari of endocytosis. Curr Biol 5:113–115.

Ramaswami M, Krishnan KS, Kelly RB (1994) Intermediates in synaptic vesicle cycling revealed by optical imaging of *Drosophila* neuromuscular junctions. Neuron 13:363–375.

Robinson PJ, Liu J-P, Powell K, Fykse EM, Sudhof T (1994) Phosphorylation of dynamin I and synaptic vesicle recycling. Trends Neurosci 17:348–353.

Rosahl T, Spillane D, Missler M, Herz J, Selig D, Wolff J, Hammer R, Malenka R, Sudhof T (1995) Essential functions of synapsin I and synapsin II in synaptic vesicle regulation. Nature 375:488–493.

Sabry JH, O'Connor TP, Evans L, Toroian-Raymond A, Kirschner M, Bentley D (1991) Microtubule behavior during guidance of pioneer neuron growth cones in situ. J Cell Biol 115:381–395.

Schulze KL, Broadie K, Perin MS, Bellen HJ (1995) Genetic and electrophysiological studies of *Drosophila* syntaxin-1A demonstrate its role in nonneuronal secretion and neurotransmission. Cell 80:311–320.

Smith DE, Fisher PA (1984) Identification, developmental regulation, and response to heat shock of two antigenically related forms of a major nuclear envelope protein in *Drosophila* embryos: application of an improved method for affinity purification of antibodies using polypeptides immobilized on nitrocellulose blots. J Cell Biol 99:20–28.

Sollner T, Bennett MK, Whiteheart SW, Scheller RH, Rothman JE (1994) A protein assembly–disassembly pathway in vitro that may correspond to sequential steps of synaptic vesicle docking, activation, and fusion. Cell 75:409–418.

Stewart BA, Atwood HA, Renger JJ, Wang J, Wu C-F (1994) Improved stability of *Drosophila* larval neuromuscular preparations in haemolymph like physiological solutions. J Comp Physiol 175:179–191.

Sudhof TC (1995) The synaptic vesicle cycle: a cascade of protein-protein interactions. Nature 375:645–653.

Sun B, Salvaterra P (1995) Two *Drosophila* nervous system antigens, Nervana 1 and 2 are homologous to the beta subunit of Na^+-K^+-ATPase. Proc Natl Acad Sci USA 92:5396–5400.

Takei K, McPherson PS, Schmid S, De Camilli P (1995) Tubular membrane invaginations coated by dynamin rings are induced by GTPγS in nerve terminals. Nature 374:186–190.

Torri-Tarelli F, Bossi M, Fesce R, Greengrad P, Valtorta P (1992) Synapsin I partially dissociates from synaptic vesicles during exocytosis induced by electrical stimulation. Neuron 9:1143–1153.

Towbin H, Staehelin T, Gordon J (1979) Electrophoretic transfer of proteins from polyacrylamide gels to nitrocellulose sheets: procedure and some applications. Proc Natl Acad Sci USA 76:4350–4354.

van de Goor J, Ramaswami M, Kelly R (1995) Redistribution of synaptic vesicles and their proteins in temperature-sensitive shibire(ts1) mutant *Drosophila*. Proc Natl Acad Sci USA 92:5739–5743.

van der Bliek A, Meyerowitz E (1991) Dynamin like protein encoded by the *Drosophila* shibire gene associated with membrane traffic. Nature 351:411–414.

Vater C, Raymond C, Ekena K, Howald-Stevenson I, Stevens T (1992) The *VPS1* protein, a homolog of dynamin required for vacuolar protein sorting in *Saccaromyces cerevisiae*, is a GTPase with two functionally separable domains. J Cell Biol 119:772–786.

Yoshikami D, Okun LM (1984) Staining of living presynaptic nerve terminals with selective fluorescent dyes. Nature 310:53–56.

Zinsmaier K, Eberle K, Buchner E, Walter N, Benzer S (1994) Paralysis and early death in cysteine string protein mutants of *Drosophila*. Science 263:977–980.